PHYSICAL REVIEW B **83**, 075306 (2011)

Bias-controlled single-electron charging of a self-assembled quantum dot in a two-dimensional-electron-gas-based *n-i*-Schottky diode

J. D. Mar,[1,2,*] X. L. Xu,[1] J. J. Baumberg,[2] F. S. F. Brossard,[1] A. C. Irvine,[3] C. Stanley,[4] and D. A. Williams[1]

[1]*Hitachi Cambridge Laboratory, Cavendish Laboratory, Cambridge CB3 0HE, United Kingdom*

[2]*NanoPhotonics Centre, Cavendish Laboratory, University of Cambridge, Cambridge CB3 0HE, United Kingdom*

[3]*Microelectronics Research Centre, Cavendish Laboratory, University of Cambridge, Cambridge CB3 0HE, United Kingdom*

[4]*Department of Electronics & Electrical Engineering, University of Glasgow, Glasgow G12 8QQ, United Kingdom*

(Received 9 December 2010; revised manuscript received 12 January 2011; published 14 February 2011)

We present bias-dependent micro-photoluminescence (μ-PL) spectroscopy of the neutral (X^0) and singly negatively-charged (X^-) excitons in single InAs/GaAs self-assembled quantum dots (QDs) embedded in the intrinsic region of an *n-i*-Schottky diode based on a two-dimensional electron gas (2DEG), which was obtained from a Si δ-doped GaAs layer. Using such a device structure, we demonstrate bias-controlled single-electron charging of a single QD as the QD *s*-shell electron state is tuned below the Fermi level. This is verified experimentally by the sequential appearance of energetically-distinct PL emission lines from the two excitons and supported by theoretical calculations. In addition, it is shown both experimentally and theoretically that simultaneous PL emission from the X^0 and X^- excitons within a particular bias range is the result of a long-lived charge-nonequilibrium state due to weak tunnel-coupling between the QDs and 2DEG in our device. Further, the ability to tune the exciton transition energies via the quantum-confined Stark effect is observed, offering insight into the carrier wave function distributions in the QD and the QD material structure. Finally, we propose a number of spintronic device concepts that may be made feasible as a result of this investigation into bias-controlled carrier tunneling between a self-assembled QD and a 2DEG.

DOI: 10.1103/PhysRevB.83.075306 PACS number(s): 73.21.La, 73.23.Hk, 78.67.Hc, 73.20.−r

I. INTRODUCTION

Due to the fully quantized electronic structure of these quasi-zero-dimensional semiconductor structures, self-assembled quantum dots (QDs) have been incorporated into quantum optoelectronic devices for applications in quantum information processing. Examples of such devices include deterministic single-photon sources,[1–4] single-QD photodiodes,[5] and charge-tunable QD diodes.[6,7] Common to all these devices is the exploitation of an increased Coulomb interaction between charge carriers when confined in such low-dimensional quantum systems, resulting in large energy shifts in the interband optical transition energies. In particular, for the field-effect charge-tunable QD devices mentioned above, sequential loading of individual electrons from a nearby Fermi sea into the QD was achieved via the Coulomb blockade effect, where the charging energy for each additional electron to tunnel was afforded by a suitable tuning of the gate voltage. However, until now, all work has used diode structures based on an *n*-type (or *p*-type) doped *bulk*-layer to realize such bias-controlled charging of QDs.[6–10]

Here, we demonstrate bias-controlled single-electron charging of single self-assembled QDs embedded in the intrinsic region of an *n-i*-Schottky diode based on a two-dimensional electron gas (2DEG). Through bias-dependent micro-photoluminescence (μ-PL) spectroscopy of a single QD, bias-controlled charging of the QD is observed as the sequential appearance of energetically-distinct PL emission lines, each corresponding to radiative recombination of either the neutral (X^0) or singly negatively-charged (X^-) QD exciton. Also, we show experimentally as well as theoretically that simultaneous PL emission from the X^0 and X^- exciton states is the result of a long-lived charge-nonequilibrium state due to slow electron tunneling between the QD and 2DEG in our device. Additionally, we show the ability to tune the exciton transition energies via the quantum-confined Stark effect (QCSE), yielding information about the carrier wave function distributions in the QD and the QD material structure. Finally, having provided an investigation of bias-controlled single-electron tunneling between a self-assembled QD and a 2DEG, we then offer a number of proposals for potential spintronic devices; namely, a spin single-electron transistor (spin-SET) and devices for electrical and optical spin-injection and -detection.

II. EXPERIMENTAL DETAILS

As shown schematically in Fig. 1, the device used in this work was designed for bias-controlled single-electron charging of single QDs and fabricated as an *n-i*-Schottky diode. From bottom to top, it consists of the following layers grown by molecular beam epitaxy (MBE) on a [100]-oriented undoped GaAs substrate: a distributed Bragg reflector (DBR) composed of 13 periods of $Al_{0.94}Ga_{0.06}As$/GaAs (67/71 nm thickness), 200 nm *i*-GaAs, followed by a Si δ-doped GaAs layer ($N_d = 5 \times 10^{12}$ cm^{-2}), from which a 2DEG forms that is confined in a V-shaped potential well[11,12] in order to serve as the Fermi sea of electrons in our *n-i*-Schottky diode. This is then followed by a single layer of InAs self-assembled QDs embedded in a 250-nm-thick *i*-GaAs layer and located 50 nm above the δ-doping. To obtain samples with a low surface-density of QDs ($\sim 10^9$ cm^{-2}), wafer rotation was stopped during MBE growth of the InAs layer.[13] The active area of the diode was defined by etching a square mesa into the sample, onto which a semitransparent Schottky contact was formed using a 10-nm-thick Ti layer. To allow for single-QD optical measurements, submicrometer-sized apertures were

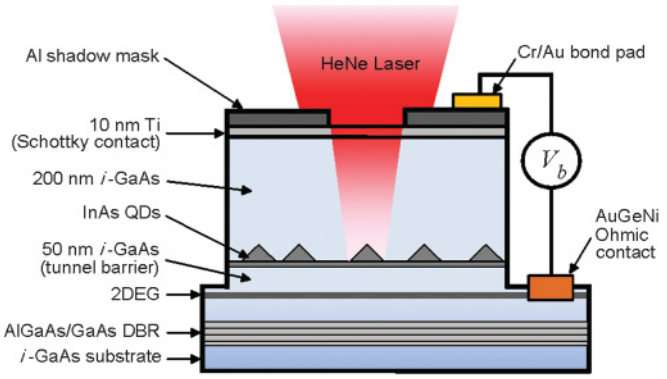

FIG. 1. (Color online) Schematic diagram of the 2DEG-based *n-i*-Schottky diode used for bias-controlled single-electron charging of single QDs in bias-dependent μ-PL spectroscopy.

etched into a near-field Al shadow mask, which was evaporated on top of the Schottky contact, via electron-beam (*e*-beam) lithography techniques. Finally, a AuGeNi ohmic contact was established to the 2DEG at a location away from the diode's active area and Cr/Au bond pads were evaporated on the ohmic contact and shadow mask to allow for connection of the diode to an external electrical circuit. The aim of incorporating the bottom DBR within the sample structure was to increase the collection efficiency of PL emission from a measured single QD. The reflection coefficient as a function of wavelength was calculated[14] and it was estimated that this DBR design should have greater than 90% reflection for light in the range of 850–930 nm, which covers the PL emission wavelength range of our QD ensemble.

Figure 2(a) presents calculations of the band-edge diagram, as well as the QD and 2DEG eigenstates, for the above *n-i*-Schottky diode structure using a one-dimensional (1D) self-consistent Poisson-Schrödinger solver. According to the results for two particular bias voltages V_b, as shown in the inset of Fig. 2(a), it is indeed possible to tune the QD *s*-shell electron level either above or below the quasi-Fermi level E_F in our device. Specifically, for $V_b = +0.2$ V, the QD electron level is positioned well above E_F, resulting in the QD being empty; whereas, for $V_b = +0.6$ V, the QD electron level has dipped below E_F, resulting in the QD being occupied electrostatically with a single electron following tunneling from the 2DEG. For this calculation, it was assumed that the QD *s*-shell exciton transition energy is ~1.34 eV, which is within the energy range of our QD ensemble.

Figure 2(b) shows calculations of the conduction band and eigenstates of the 2DEG, which was derived from the Si δ-doping. It reveals a V-shaped conduction-band profile, which is due to the δ-function-like distribution of positive ionized impurities, with four confined two-dimensional (2D) quantized subbands whose eigenvalues E_0, E_1, E_2, and E_3 are shown along with their respective wave function probability distributions. It is important to note that, particularly for the higher-order subbands, the spatial extent of the delocalization of electrons from their ionized donor impurities and the spreading-out of electronic states is much larger compared to that of the localized δ-function-like ionized impurity profile, which is similar to the GaAs lattice constant.[11] Therefore, electron mobilities and the effects of ionized impurity scattering in such 2DEGs formed from δ-doping is expected to be similar to those in 2DEGs formed from modulation-doped heterostructures.[15]

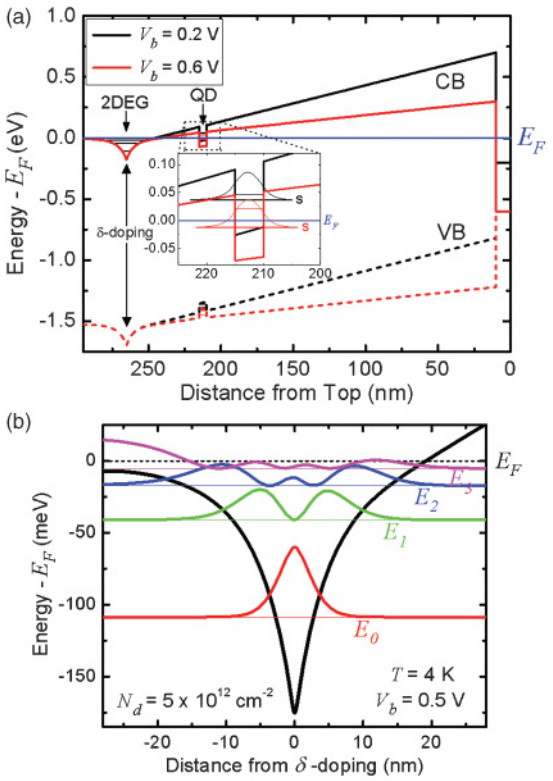

FIG. 2. (Color online) Theoretical calculations of (a) the conduction band (solid lines), valence band (dashed lines), and QD and 2DEG eigenstates for the *n-i*-Schottky diode, showing the ability to tune the QD *s*-shell electron state above ($V_b = +0.2$ V) or below ($V_b = +0.6$ V) the Fermi energy E_F, as seen in the inset, and (b) the V-shaped conduction band (black line) and 2DEG eigenvalues (E_0, E_1, E_2, E_3) and respective probability distributions for the four confined 2D subbands, which are the result of the Si δ-doping ($N_d = 5 \times 10^{12}$ cm^{-2}).

The samples were measured using a μ-PL system, where nonresonant optical excitation from the output of a HeNe laser ($\lambda = 632.8$ nm) was focused on a given aperture using a microscope objective lens [numerical aperture (NA) = 0.5], which was mounted on a piezo-driven *xyz*-stage for precise nanopositioning. μ-PL measurements on the sample were performed at low temperatures (~4.2 K) in a He-flow cold-finger optical cryostat and the bias voltage was supplied by a commercial source-measure unit (SMU). PL emission from the sample was collected by the same objective lens and dispersed in a 0.55-m spectrometer equipped with a liquid-nitrogen-cooled InGaAs CCD detector array.

III. RESULTS AND DISCUSSION

Bias-dependent μ-PL measurements were performed on several single QDs, each isolated in an aperture with a diameter of ~300 nm. Figure 3(a) presents a contour plot of the time-integrated μ-PL spectra from one particular QD for the bias range of $0.3\ \text{V} \leqslant V_b \leqslant 0.6$ V with a laser excitation intensity of ~4.2 μW, while Fig. 3(b) displays the single-QD

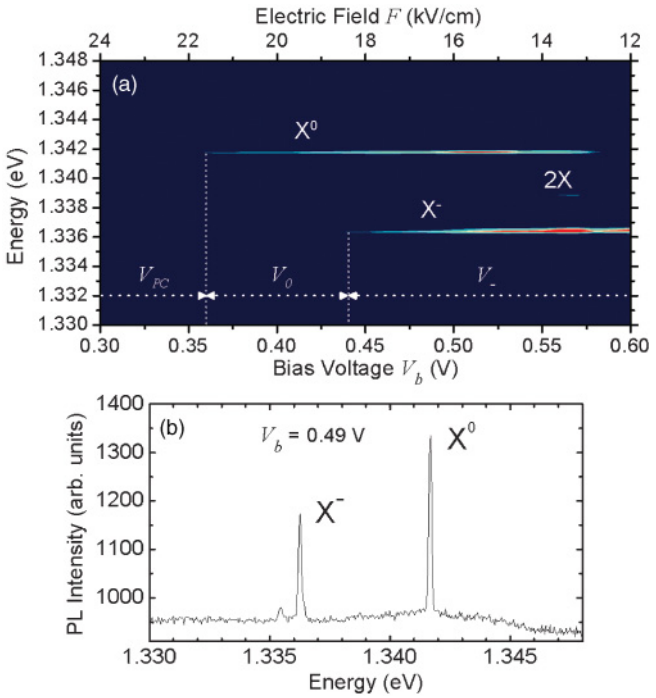

FIG. 3. (Color online) (a) Contour plot of the bias-dependent μ-PL spectra of a single QD, showing PL emission lines from X^0, X^-, and $2X$. (b) Single-QD μ-PL spectrum for $V_b = 0.49$ V.

spectrum for $V_b = 0.49$ V. Figure 3(a) is characterized by the appearance of three distinct PL emission lines over the measured bias range and their assignments to X^0, X^-, and the biexciton state ($2X$) will be discussed in this section. Through laser-intensity-dependent measurements of the integrated PL intensity for each of the PL emission lines observed in Fig. 3(a), it was confirmed that the two strong lines at ~1.342 and ~1.336 eV originate from single-exciton states, while the weak line at ~1.339 eV originates from $2X$—the neutral two-exciton state occupying the QD s-shell. In our device, the electric field F at the QD layer is defined as[11,15] $F = (V_i - V_b)/d$, where V_i is the intrinsic built-in potential (Schottky barrier) and d is the distance between the Si δ-doping and Schottky contact. V_i was determined by measuring the value of V_b at which the photocurrent (PC) signal changed sign (i.e., at the flat-band condition) for nonresonant laser excitation using a HeNe laser. It is important to note that a motivation for choosing δ-doping, as opposed to other approaches (e.g., a modulation-doped heterostructure), to obtain the 2DEG in our device was the ease of determining the electric field at the QD layer and its linearity as a function of bias voltage.[11,15]

A. Bias-controlled single-electron charging

Studying the appearance and relative intensities of the observed PL emission lines as a function of V_b provides insight into the bias-dependent carrier dynamics and coupling strength between the 2DEG and QD. With this in mind, Fig. 3(a) can be divided into three bias ranges, labeled as V_{PC}, V_0, and V_-. For the V_{PC} bias range ($V_b < 0.36$ V), the QD s-shell electron state is well above E_F and thus the QD is empty prior to laser excitation. Then, as an exciton is captured in the QD following laser excitation, the high electric-field conditions here lead to exciton ionization on a time scale much shorter than the exciton recombination time (~1 ns),[16] which is independent of electric field, as the electron and hole tunnel out of the QD and toward the 2DEG and Schottky contact, respectively. Therefore, no PL emission from the QD is observed in this bias range and instead a PC is generated. Next, for the V_0 bias range ($0.36\ \text{V} \leqslant V_b < 0.44$ V), a PL emission line appears at ~1.342 eV. Here, the s-shell electron state is still above E_F and thus the QD remains uncharged prior to laser excitation. However, upon capture and subsequent relaxation of a single exciton into the QD s-shell under such low electric-field conditions, radiative recombination of the exciton is permitted as the electron tunneling time out of the QD is now longer than the exciton recombination time. Therefore, the PL emission line at ~1.342 eV is assigned to X^0. Finally, for the V_- bias range ($V_b \geqslant 0.44$ V), a second PL emission line appears at ~1.336 eV. For this case, the s-shell electron state has dipped below E_F and, consequently, the QD is charged with a single electron that has tunneled from the 2DEG into the QD. Due to the Coulomb blockade effect, a second electron with opposite spin is prevented from tunneling into the s-shell electron state, unless the charging energy is afforded through a further increase in the forward bias voltage. Now, the capture and relaxation of a single exciton into the QD s-shell results in the formation of X^-, which consists of two electrons in a spin singlet and one hole with either spin. Therefore, as the carrier tunneling time is much longer than the exciton recombination time in this bias range, the decay of X^- creates a photon with the X^- transition energy, observed as the PL emission line at ~1.336 eV that is redshifted with respect to the X^0 emission line. The presence of the electrostatically-induced s-shell electron causes a renormalization of the exciton transition energies, which, in the case of the X^- few-particle state, is due to the electron-hole (e-h) Coulomb attraction outweighing the electron-electron (e-e) Coulomb repulsion.[17] The renormalization energy is ~5 meV for this particular QD, comparable to those reported in other works on similar QDs.[6,7,10] Also, neither for this QD nor any of those measured throughout our sample did we observe PL emission from higher-order charged exciton states (e.g., X^{2-}, X^{3-}, etc.), which have been reported in other works.[6,7,10] Considering that our QDs possess a relatively small confinement potential (~50 meV), this is most likely due to the fact that, as V_b is increased, flat-band conditions are met before the charging energy required for a second electron to tunnel is afforded and the wetting layer becomes flooded with electrons[5] from the 2DEG.

Theoretical calculations of the s-shell electron state energy relative to E_F were performed for this QD as a function of V_b using a 1D self-consistent Poisson-Schrödinger solver. As seen in the results plotted in Fig. 4, the bias voltage at which the electron state is equal to E_F (i.e., V_b at the onset of single-electron charging of the QD) coincides remarkably well with the appearance of the X^- PL emission line in the experimental measurements of Fig. 3(a).

While the 2DEG consists of electron energy levels that are quantized into 2D subbands, we did not observe any evidence of strong coupling through coherent tunneling between the QD and 2DEG electron energy levels that would result in

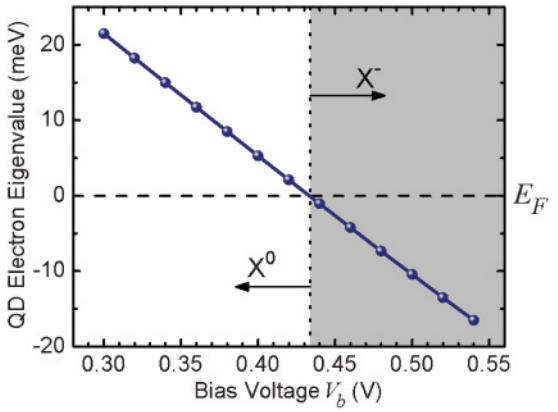

FIG. 4. (Color online) Calculated QD *s*-shell electron state energy relative to E_F as a function of V_b. The gray-shaded region represents the bias range where the electron state is below E_F, resulting in single-electron charging of the QD and subsequent X^- PL emission.

the formation of molecular states when tuned into resonance, as was observed in other works having two coupled QDs separated by a narrow tunnel barrier.[18–21] This is due to our sample's much wider tunnel barrier compared to those in reports on coupled QDs,[18–21] as supported by the calculated electronic wave function probability distributions in our sample when the QD *s*-shell electron level is tuned into resonance with the highest-order (E_3) and second-highest-order (E_2) 2DEG subbands, shown in Figs. 5(a) and 5(b), respectively. Furthermore, there was no observation of PL emission from any X^- triplet states, whose PL energies would have been separated energetically from that of the observed X^- singlet state[19,22] (two electrons in a spin-singlet). The existence of

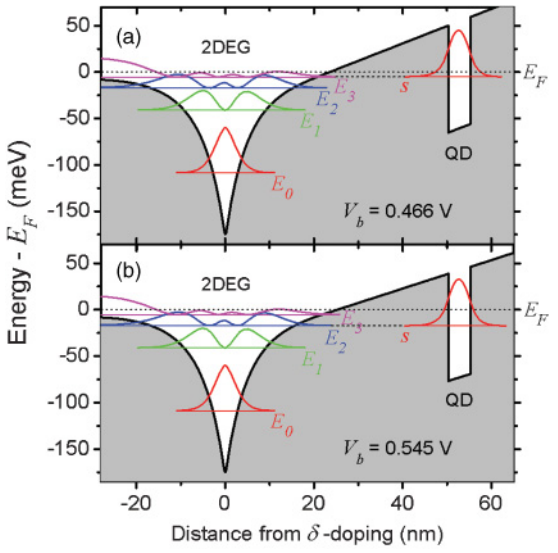

FIG. 5. (Color online) Calculated electronic wave function probability distributions for V_b, where the QD *s*-shell electron state is in resonance with the (a) highest-order (E_3) and (b) second-highest-order (E_2) 2DEG subbands, showing the absence of strong tunnel-coupling between the QD and 2DEG. Corresponding calculations for the lower-order subbands, which have wider tunnel barriers due to the V-shaped conduction-band profile, lead to the same conclusion.

X^- triplet states would have been expected only in the case of strong tunnel-coupling as one electron from each of the QD and 2DEG would form a molecular state,[18,19] while two electrons in the QD can only exist in a spin-singlet as required by the Pauli exclusion principle.

B. Simultaneous X^- and X^0 PL emission

In light of the above discussion, a surprising feature of the bias-dependent PL spectra in Fig. 3(a) is PL emission from X^0 within the V_- bias range, where emission from only X^- is expected. The existence of X^0 PL emission is the result of a long-lived charge-nonequilibrium state, where the QD does not possess a net charge of one electron—rather, a net charge of zero – despite the electron state being below E_F. Given the relatively thick tunnel barrier in our device (33 nm),[23] compared to other works [25 nm (Refs. 6 and 7) and 16 nm (Ref. 10)], which did not report simultaneous PL emission from X^0 and X^-, such a long-lived charge-nonequilibrium state is due to weak tunnel-coupling between the QD and 2DEG and is created by means of two possible processes within the V_- bias range. First, as illustrated schematically in Fig. 6(a), since excitons are formed in the QD via capture and relaxation of carriers optically-excited into the GaAs matrix, it is possible that only a single hole is captured in the QD, thereby creating a X^0 with the electrostatically-induced resident single electron. If the tunneling rate of a second electron from the 2DEG into the QD to restore charge-equilibrium is much slower than the exciton recombination rate ($\sim$1 ns^{-1}),[16] this X^0 will radiatively recombine, resulting in the emission of a photon with the X^0 transition energy, assuming that a bright exciton had been formed. Alternatively, while the laser excitation used here is linearly-polarized, an equal number of spin-up and spin-down carriers is optically-generated in the GaAs matrix and hence also in the QD upon capture and relaxation.[24] Then, if the electron captured by the QD has the same spin as the electrostatically-induced electron, it will remain in the QD *p*-shell due to Pauli blocking. Consequently, this *p*-shell electron may quickly tunnel out of the QD through its small tunnel barrier if its spin-flip time to the QD *s*-shell is longer than its tunneling time to the 2DEG, as illustrated in Fig. 6(b). Therefore, if the tunneling rate of an electron from the 2DEG into the QD to restore charge-equilibrium is much slower than the recombination rate, the outcome is the radiative recombination of a X^0 in the QD, assuming the exciton is bright.

To support the above discussion, we calculate the electron tunneling rate as a function of the bias-dependent tunnel barrier height, and show that the long-lived charge-nonequilibrium state in our device is the result of a slow electron tunneling rate from the 2DEG into the QD to restore charge-equilibrium compared to the bias-independent exciton recombination rate R_{PL} ($\sim$1 ns^{-1}).[16] The electron tunneling rate R_T between the 2DEG and QD can be modeled via a 1D Wentzel-Kramers-Brillouin (WKB) approximation,[25]

$$R_T = \frac{\hbar\pi}{2m_e^* H^2} \exp\left(\frac{-4z}{3\hbar}\sqrt{2m_e^* E_b}\right), \qquad (1)$$

where z is the tunnel barrier width, H is the QD height, E_b is the tunnel barrier height, m_e^* is the electron effective

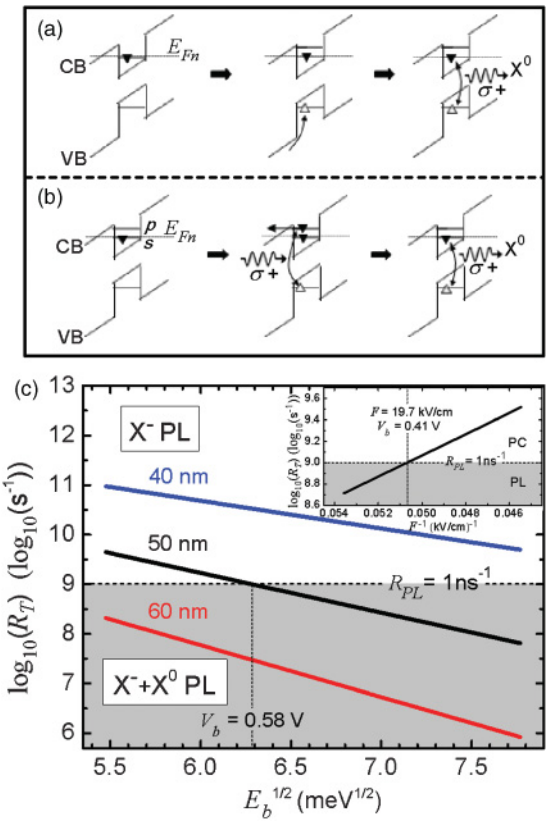

FIG. 6. (Color online) Schematic diagram of X^0 formation within the V_- bias range via (a) capture of a single hole and (b) p-shell electron tunneling out of the QD. Filled (open) triangles represent electrons (holes) with a given spin, as indicated; σ^+ refers to optical excitation of a QD exciton with a spin-down (spin-up) electron (hole). (c) Calculated electron tunneling rate R_T as a function of tunnel barrier height E_b within the V_- bias range for our present device (50-nm separation between QD and δ-doping; black line) and for two hypothetical devices that differ from the first device by only the QD to δ-doping separation: 40 nm (blue line) and 60 nm (red line). Inset: R_T as a function of F within the V_0 bias range for the 50-nm device.

mass in GaAs, and $\hbar$ is the reduced Planck's constant. As presented in Fig. 6(c), R_T has been calculated as a function of E_b within the V_- bias range for our device,[26] which has a 50-nm separation between δ-doping and the QD layer, as well as for two hypothetical devices that differ from our present device by only the separation of their δ-doping and QD layers (40 and 60 nm). The grey- (non-) shaded region represents a situation where R_T (R_{PL}) is slower than R_{PL} (R_T), resulting in X^- and X^0 (X^- only) PL emission. It is clear from Fig. 6(c) that the tunnel barrier width has a strong influence on R_T and hence also on the probability of restoring charge-equilibrium via tunneling of an electron from the 2DEG into the QD. For example, the 60- (40-) nm device is expected to exhibit PL emission from X^- and X^0 (X^- only) throughout the V_- bias range. However, for our 50-nm device, simultaneous PL emission from X^0 and X^- is expected only toward larger E_b; whereas, only X^- PL emission is expected as E_b is decreased (i.e., V_b is increased) sufficiently, since there is now a higher probability of an electron tunneling into the QD to restore charge-equilibrium prior to recombination. According to the theoretical model, this transition occurs at $V_b = 0.58$ V, which agrees very well with the quenching of X^0 PL emission observed in the experimental results of Fig. 3(a). Finally, by substituting $z = E_b/eF$ into Eq. (1) (where e is the elementary charge), we use this model to calculate R_T as a function of F within the V_0 bias range, noting that now the tunnel barrier width is dependent on bias voltage. We find that the value of V_b at which quenching of X^0 PL emission was experimentally observed in Fig. 3(a), which is due to the optically-excited electron tunneling out of the QD prior to exciton recombination, agrees reasonably well with the theoretical prediction shown in the inset of Fig. 6(c).

C. Competition between tunneling and spin-flipping of QD p-shell electron

An interesting feature can be found within the V_- bias range (specifically, 0.44 V $\leqslant V_b \leqslant$ 0.58 V) of Fig. 3(a) by examining the relative PL intensities of X^0 and X^- as a function of V_b, which is given in the plot of Fig. 7(a). Each plotted value of PL intensity in this figure is proportional to the area under a Lorentzian curve fit to the corresponding emission peak of the time-integrated PL spectrum. The plot reveals two ranges within V_-: a low-bias range characterized by dominant X^0 emission, followed by a high-bias range characterized by dominant X^- emission, with the transition

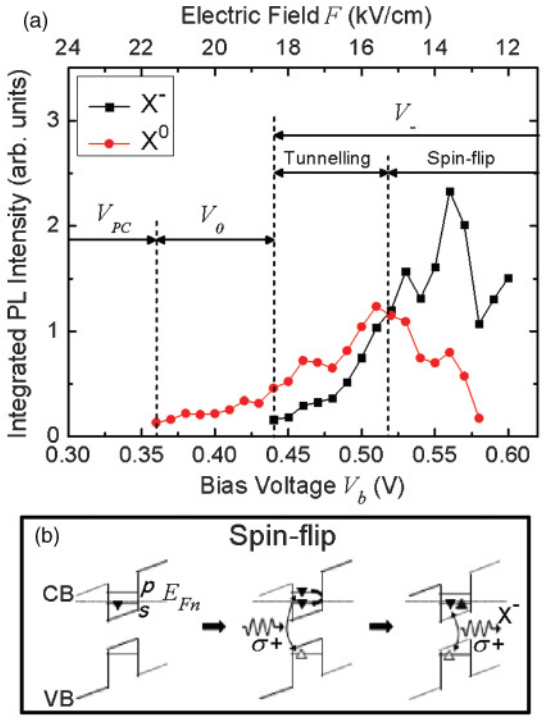

FIG. 7. (Color online) (a) Integrated PL intensities of X^0 and X^- as a function of V_b, showing bias ranges for dominant X^0 (X^-) PL emission within the V_- bias range due to a higher probability of QD p-shell electron tunneling (spin-flipping). (b) Schematic diagram of X^- formation and radiative recombination via a p-shell electron spin-flip under low electric-field conditions. Filled (open) triangles represent electrons (holes) with a given spin, as indicated; σ^+ refers to the excitation or recombination of a QD exciton with a spin-down electron and spin-up hole.

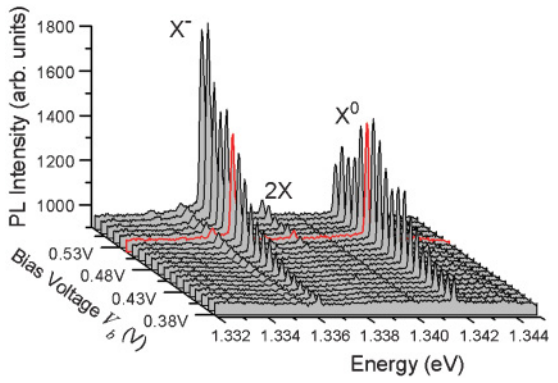

FIG. 8. (Color online) μ-PL spectra for a series of V_b, showing the transition point (red trace) at $V_b = 0.52$ V between dominant X^0 and X^- integrated PL intensity.

point occurring at $V_b = 0.52$ V. The existence of these two distinct ranges within V_- can be explained by considering the possible processes leading to the formation of either X^0 or X^-. The processes leading to X^0 formation are as follows: (1) single-hole capture into the QD [Fig. 6(a)] and (2) capture of an electron-hole pair into the QD, where the electron remains in the QD p-shell due to Pauli blocking and subsequently tunnels quickly out of the QD [Fig. 6(b)]. On the other hand, the processes leading to X^- formation are as follows: (3) capture of an electron-hole pair into the QD with the electron having opposite spin to the electrostatically-induced resident electron and (4) capture of an electron-hole pair into the QD where the electron, which is initially Pauli-blocked in the p-shell, undergoes a spin-flip before the possibility of tunneling out, and consequently relaxes into the QD s-shell [Fig. 7(b)]. Unlike processes (1) and (3), the probability of process (2) occurring is dependent on the bias voltage (electric-field conditions). Also, while the electron spin-flip time is essentially independent of the electric-field conditions, the probability of process (4) occurring is dependent on the p-shell electron tunnelling time with respect to the spin-flip time. Therefore, the transition between dominant X^0 and dominant X^- within V_- is the result of competition between the tunnelling and spin-flipping processes that may be experienced by the Pauli-blocked p-shell electron depending on the electric-field conditions. Referring to Fig. 7(a), we conclude that the event of tunneling (spin-flipping) of the p-shell electron is more probable for $V_b < 0.52$ V ($V_b > 0.52$ V), as can be seen also in Fig. 8 showing PL spectra for a series of V_b about the transition point. Using the theoretical model of Eq. (1) along with the calculated tunnel barrier height for the p-shell electron, we estimate the QD p-shell electron tunneling time to be ~50 ps at the $V_b = 0.52$ V transition point, where the tunneling time is comparable to the spin-flip time.

It is worth noting that the gradual increase in PL intensity with increasing forward bias is due to a general decrease in the ionization and tunneling rate of excitons out of the QD. Also, as seen in Figs. 3(a) and 8, the appearance of the $2X$ emission line coincides with the dominant X^- bias range, which is expected since the formation of $2X$ in this bias range requires the capture of only a single hole. Further, this effect is enhanced in our device due to the increased supply of optically-generated holes

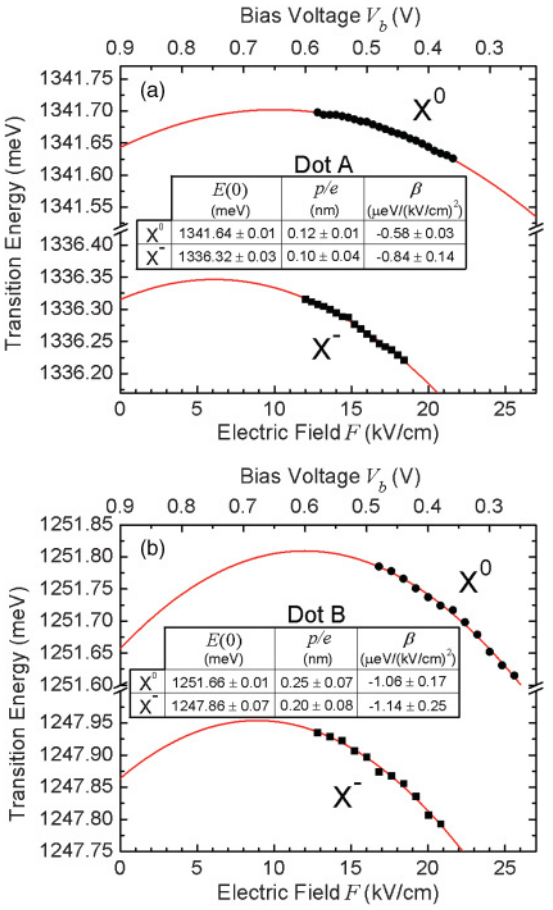

Dot A	$E(0)$ (meV)	p/e (nm)	β (μeV/(kV/cm)^2)
X^0	1341.64 ± 0.01	0.12 ± 0.01	-0.58 ± 0.03
X^-	1336.32 ± 0.03	0.10 ± 0.04	-0.84 ± 0.14

Dot B	$E(0)$ (meV)	p/e (nm)	β (μeV/(kV/cm)^2)
X^0	1251.66 ± 0.01	0.25 ± 0.07	-1.06 ± 0.17
X^-	1247.86 ± 0.07	0.20 ± 0.08	-1.14 ± 0.25

FIG. 9. (Color online) X^0 and X^- transition energies as a function of electric field with fits (red curve) using Eq. (2) for (a) Dot A and (b) Dot B. The fit results for $E(0)$, p, and β are given in the tables for each QD.

from the relatively thick 50-nm GaAs layer between the QD and δ-doping, compared to other works.[6,7,10]

D. Quantum-confined Stark effect

We now demonstrate the ability to tune the X^0 and X^- transition energies with vertical electric field (bias voltage) via the QCSE, which is the result of an electric-field-controlled exciton dipole moment in the QD. The X^0 and X^- transition energies for the QD presented thus far, which we now refer to as Dot A, are plotted in Fig. 9(a) as a function of vertical electric field F; meanwhile, those for another QD in the same sample (Dot B), which is redshifted by ~90 meV with respect to Dot A, are plotted in Fig. 9(b). The plotted values for the transition energies were determined by taking the center of a Lorentzian curve fit to the corresponding PL emission peak, while the sign convention for F is such that positive fields point from substrate to Schottky contact, following the definition of F given earlier.

The dependence of the exciton transition energy on vertical electric field F can be described accurately by[27,28]

$$E(F) = E(0) + pF + \beta F^2, \tag{2}$$

where $E(0)$ is the exciton transition energy at $F = 0$, p is the permanent exciton dipole moment in the vertical (growth)

direction, and β is the exciton polarizability. As shown in the tables in Fig. 9, fitting this model to the experimental data yields values for $E(0)$, p, and β for both X^0 and X^- in Dots A and B.

The fit results for Dots A and B lead to several conclusions regarding the electron and hole wave functions in the QDs due to the QD material structure, confinement potential, and Coulomb interactions in the X^- few-particle state. First, the positive sign of p for both QDs indicates that the center-of-gravity of the electron wave function is localized above that of the hole in the QD. This dipole alignment is consistent with theoretical calculations on pure InAs self-assembled QDs with a pyramidal shape[29–32] and is opposite to those in other works on QDs showing an inverted alignment[27,33] that is due to In-enrichment toward the QD apex.[27] Second, the slight decrease of p for X^- relative to X^0 in both QDs suggests that the centers-of-gravity of the electron and hole wave functions move closer together when an electron is added to the QD. This effect is similar to that observed in Ref. 33 with X^0 and X^+ (positively-charged exciton) as a hole was added to the QD. Third, since the magnitude of β is correlated with the QD height,[34] the larger β observed for Dot B compared to Dot A implies that Dot B possesses an increased height. Since the quantization energy is inversely proportional to the QD height, this is supported by the fact that the transition energy of Dot B is redshifted relative to that of Dot A by ~90 meV. Finally, since the magnitude of p decreases with increasing truncation of the QD,[34] the smaller p for Dot A relative to Dot B indicates that Dot A is more truncated.

E. Proposals for spintronic devices

In this article, we have provided a detailed investigation of single-electron tunneling between a single self-assembled QD and a 2DEG in a field-effect device. Using a sample structure similar to that presented in this work, we now propose a series of device concepts for applications in spintronics that may be made feasible as a result of our investigation. As will be shown in the following, the proposed devices that are coupled to optical fields are made possible only through the use of self-assembled QDs, which are known to exhibit a high optical quality due to their relatively defect-free crystal structure.

(a) *Spin single-electron transistor (spin-SET).* As seen in Fig. 10(a), the structure of the spin-SET is similar to that of the well-known Datta-Das transistor,[35] except for several

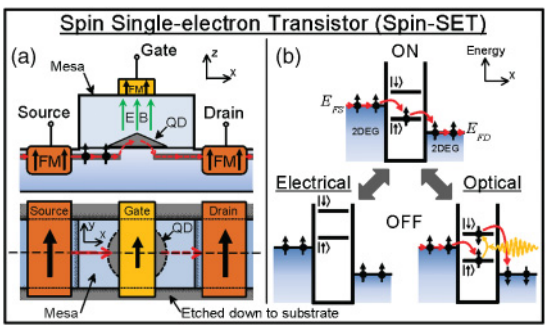

FIG. 10. (Color online) Spin-SET proposal showing (a) the device structure and (b) the corresponding energy-level diagrams for electrical and optical gating.

crucial differences. First, our spin-SET consists of a single self-assembled QD that is located above and tunnel-coupled to the nearby 2DEG, just as in the device already examined throughout this work. In addition, the single QD is spatially-isolated from other QDs by etching the sample around it to form a mesa. Second, a ferromagnetic (FM) Schottky gate, which is positioned directly above the QD and made narrower than the QD diameter, depletes the 2DEG directly below through the application of a suitable negative gate voltage V_g such that the conductivity in the 2DEG channel below the QD is zero. Therefore, while QD-2DEG tunnel-coupling toward the edges of the QD is maintained, electron transport from source to drain is permitted only via the single QD for an appropriate V_g and drain-to-source voltage V_{ds}. The FM gate also serves to establish a local magnetic field to Zeeman-split the QD spin-states. While an electron g-factor of ~0.8 has been reported for InAs self-assembled QDs,[36] Zeeman-splittings of ~10 μeV should be possible for a stray magnetic field of 200 mT from an Fe top gate.[37] Additionally, the QD energy levels are designed such that depletion of the 2DEG and QD-2DEG tunnel-coupling are maintained while the s-shell electron state is tuned through the Fermi levels of the source (E_{FS}) and drain (E_{FD}) as V_g is modulated. Further, the sample is etched down to the substrate except for those regions that define the 2DEG source and drain in the x-y plane [blue area, bottom diagram of Fig. 10(a)]. Energy-level diagrams of the spin-SET in the x-direction are shown in Fig. 10(b). As shown in the top diagram of Fig. 10(b), for a FM source (drain) that injects (transmits) spin-up electrons and a positive V_{ds}, the spin-SET is turned on (i.e., nonzero drain-to-source current I_{ds}) if the QD spin-up electron state is energetically-positioned below E_{FS} and above E_{FD}. Here, a spin-up electron is thus permitted to tunnel from source to drain via the QD, assuming no spin relaxation occurs. The spin-SET can then be gated-off electrically by setting V_g such that the spin-up state is positioned well above E_{FS}, resulting in zero I_{ds} as no electrons are permitted to tunnel into the QD and hence to the drain. Alternatively, the spin-SET can be gated-off *optically* by performing a π-rotation of the QD spin using an ultrafast laser pulse via the optical Stark effect,[38] leading to zero I_{ds} as spin-down electrons would reflect, rather than transmit, upon arrival at the FM drain. Although Fig. 10 illustrates the operation of a spin-SET for spin-up electrons, it is worth noting that the same can be achieved for spin-down electrons. Finally, the purpose of the local magnetic field here is to Zeeman-split the QD spin-states and thus increase the spin relaxation time while the electron resides in the QD.

(b) *Electrical spin-injection and -detection.* As seen in Fig. 11(a), the structure of our proposed device for electrically-gated spin-injection and -detection is similar to that of the above spin-SET. However, since the objective here is to inject (detect) a given electron spin into (from) another spintronic device, the differences between this device and the spin-SET are that there is only one ohmic contact to the 2DEG and that this contact can be nonmagnetic. Using this device for the spin-injection of spin-up (spin-down) electrons, V_g is set such that only the spin-up (spin-down) QD electron state is energetically-positioned between the contact Fermi level and the 2DEG Fermi level on the right-hand side of the QD, as illustrated in the top two diagrams of Fig. 11(b). On the

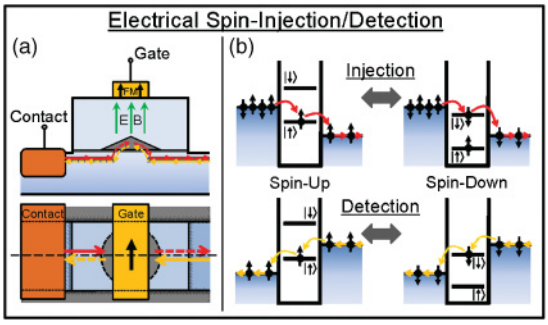

FIG. 11. (Color online) Electrical spin-injection and spin-detection device proposal showing (a) the device structure and (b) the corresponding energy-level diagrams for injection and detection of spin-up and spin-down electrons.

other hand, using this device for the spin-detection of spin-up (spin-down) electrons, V_g is set such that only the spin-up (spin-down) QD electron state is energetically-positioned between the contact Fermi level and the 2DEG Fermi level on the right-hand side of the QD, as illustrated in the bottom two diagrams of Fig. 11(b). Therefore, the arrival of a spin current at the device will be measured as a charge current at the contact. Finally, by ignoring the contact on the left-hand side of the QD, it is worth noting that this device can also function as a spin-filter within a spintronic circuit.

(c) *Optical spin-injection and -detection.* As seen in Fig. 12(a), the structure of the proposed device for optical spin-injection and -detection is similar to that for electrical spin-injection and -detection. However, the only differences here are that there is no electrical contact and that the top gate completely shadows the QD except toward only the right-hand edge where QD-2DEG tunnel-coupling remains present. Here, the top gate is made from a p-type dilute magnetic semiconductor (DMS), such as GaMnAs, in order to provide hole carriers with a known spin to the QD and also to serve as a ferromagnetic gate that Zeeman-splits the QD spin-states due to its stray magnetic field. For optical spin-injection, V_g is tuned such that both QD electron (hole) spin-states are energetically-positioned above (below) the Fermi level in the 2DEG (p-type layer). Then, for optical injection of a spin-up electron [left-hand diagram of Fig. 12(b)], an exciton is resonantly-excited in the QD using σ^- circularly-polarized

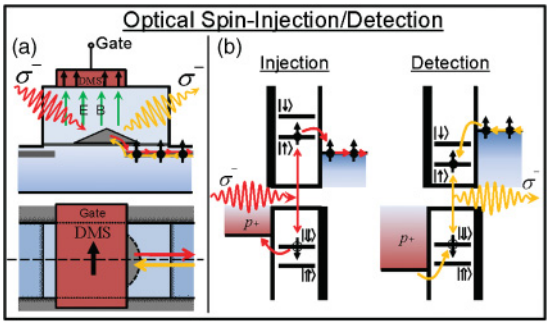

FIG. 12. (Color online) Optical spin-injection and spin-detection device proposal showing (a) the device structure and (b) the corresponding energy-level diagrams for injection and detection of spin-up electrons.

light to create a spin-up (spin-down) electron (hole). This can be achieved, for example, by using an ultrafast laser π-pulse that performs an inversion of the QD exciton two-level system.[39,40] Subsequently, the spin-up electron is injected into the 2DEG as it tunnels out of the QD, while the hole tunnels out toward the p-type layer. On the other hand, for optical spin-detection, V_g is tuned such that both QD electron (hole) spin-states are energetically-positioned below (above) the Fermi level in the 2DEG (p-type layer). Then, in the optical detection of a spin-up electron [right-hand diagram of Fig. 12(b)], a photon will be emitted from the QD only if a spin-up electron from the 2DEG radiatively recombines with the spin-down hole from the DMS gate, which is magnetized in such a way that its magnetic moment results in the injection of spin-down hole carriers into the QD.

In the device proposals throughout this section, it is important to note that we have made two idealistic assumptions. First, we have assumed ideal ferromagnetic contacts that inject or transmit only the majority spins and that there is no relaxation of spin polarization at the interfaces due to scattering events. Second, we have assumed no scattering-induced spin relaxation in the 2DEG via either the Elliott-Yafet[41] or D'yakonov-Perel'[42] (DP) spin relaxation mechanisms as a result of spin-orbit coupling. Specifically, in the case of DP relaxation, we have presupposed the absence of inversion asymmetry due to stray electric fields from the gate or a lack of a center of inversion in the GaAs zincblende crystal structure, which would lead to Rashba and Dresselhaus spin-orbit interactions, respectively. Note also that, since the current-driving electric field and carrier velocity in the 2DEG are along the same direction, this electric field should not result in Rashba spin-orbit interaction.

IV. CONCLUSIONS

We have demonstrated bias-controlled single-electron charging of single QDs in a 2DEG-based n-i-Schottky diode. Through bias-dependent μ-PL spectroscopy of single QDs, we have observed such bias-controlled charging as the sequential appearance of energetically-distinct PL emission lines, each corresponding to radiative recombination of either X^0 or X^-. Also, it was shown experimentally and supported theoretically that simultaneous PL emission from X^0 and X^- is the result of a long-lived charge-nonequilibrium state due to weak tunnel-coupling between the 2DEG and QD. Then, the QCSE was observed through the ability to tune the exciton transition energies with vertical electric field, providing insight into the electron and hole wave function distributions in the QD and QD material structure. Finally, having given a comprehensive investigation into electron tunnel-coupling between a self-assembled QD and a 2DEG in a field-effect device, we proposed several concepts for future spintronic devices that could be made feasible as a result of our investigation.

ACKNOWLEDGMENTS

J.D.M. gratefully acknowledges financial support from HEFCE, CCT, and NSERC (PGS M, PGS D).

*Author to whom correspondence should be addressed. jm585@cam.ac.uk.

[1] P. Michler, A. Kiraz, C. Becher, W. V. Schoenfeld, P. M. Petroff, Lidong Zhang, E. Hu, and A. Imamoğlu, Science **290**, 2282 (2000).

[2] J. Kim, O. Benson, H. Kan, and Y. Yamamoto, Nature (London) **397**, 500 (1999).

[3] X. L. Xu, I. Toft, R. T. Phillips, J. Mar, K. Hammura, and D. A. Williams, Appl. Phys. Lett. **90**, 061103 (2007).

[4] X. L. Xu, D. A. Williams, and J. R. A. Cleaver, Appl. Phys. Lett. **85**, 3238 (2004).

[5] F. Findeis, M. Baier, E. Beham, A. Zrenner, and G. Abstreiter, Appl. Phys. Lett. **78**, 2958 (2001).

[6] R. J. Warburton, C. Schäflein, D. Haft, F. Bickel, A. Lorke, K. Karrai, J. M. Garcia, W. Schoenfeld, and P. M. Petroff, Nature (London) **405**, 926 (2000).

[7] J. J. Finley, P. W. Fry, A. D. Ashmore, A. Lemaître, A. I. Tartakovskii, R. Oulton, D. J. Mowbray, M. S. Skolnick, M. Hopkinson, P. D. Buckle, and P. A. Maksym, Phys. Rev. B **63**, 161305(R) (2001).

[8] A. Högele, S. Seidl, M. Kroner, K. Karrai, R. J. Warburton, B. D. Gerardot, and P. M. Petroff, Phys. Rev. Lett. **93**, 217401 (2004).

[9] B. D. Gerardot, D. Brunner, P. A. Dalgarno, P. Öhberg, S. Seidl, M. Kroner, K. Karrai, N. G. Stoltz, P. M. Petroff, and R. J. Warburton, Nature (London) **451**, 441 (2008).

[10] N. A. J. M. Kleemans, J. van Bree, A. O. Govorov, J. G. Keizer, G. J. Hamhuis, R. Nötzel, A. Yu. Silov, and P. M. Koenraad, Nat. Phys. **6**, 534 (2010).

[11] K. Ploog, J. Cryst. Growth **81**, 304 (1987).

[12] L. M. R. Scolfaro, R. P. Camata, J. M. V. Martins, and J. R. Leite, Superlattices Microstruct. **12**, 203 (1992).

[13] D. Leonard, K. Pond, and P. M. Petroff, Phys. Rev. B **50**, 11687 (1994).

[14] The refractive indices were assumed to be 2.95 and 3.51 for $Al_{0.94}Ga_{0.06}As$ and GaAs, respectively, at 4.2 K.

[15] E. F. Schubert, A. Fischer, and K. Ploog, IEEE Trans. Electron Devices **ED-33**, 625 (1986).

[16] R. Heitz, A. Kalburge, Q. Xie, M. Grundmann, P. Chen, A. Hoffmann, A. Madhukar, and D. Bimberg, Phys. Rev. B **57**, 9050 (1998).

[17] S. Rodt, A. Schliwa, K. Pötschke, F. Guffarth, and D. Bimberg, Phys. Rev. B **71**, 155325 (2005).

[18] E. A. Stinaff, M. Scheibner, A. S. Bracker, I. V. Ponomarev, V. L. Korenev, M. E. Ware, M. F. Doty, T. L. Reinecke, and D. Gammon, Science **311**, 636 (2006).

[19] M. F. Doty, M. Scheibner, I. V. Ponomarev, E. A. Stinaff, A. S. Bracker, V. L. Korenev, T. L. Reinecke, and D. Gammon, Phys. Rev. Lett. **97**, 197202 (2006).

[20] D. Kim, S. E. Economou, S. C. Badescu, M. Scheibner, A. S. Bracker, M. Bashkansky, T. L. Reinecke, and D. Gammon, Phys. Rev. Lett. **101**, 236804 (2008).

[21] X. Xu, A. Andreev, D. A. Williams, and J. R. A. Cleaver, Appl. Phys. Lett. **89**, 091120 (2006).

[22] M. Scheibner, M. F. Doty, I. V. Ponomarev, A. S. Bracker, E. A. Stinaff, V. L. Korenev, T. L. Reinecke, and D. Gammon, Phys. Rev. B **75**, 245318 (2007).

[23] The tunnel barrier width of 33 nm in our device was calculated using a 1D self-consistent Poisson-Schrödinger solver (see Fig. 2) and is due to the V-shaped conduction-band profile as a result of the δ-doping.

[24] Using circularly-polarized nonresonant laser excitation above the GaAs band gap would also result in an equal number of spin-up and spin-down carriers relaxing into the QDs [see Y. Toda, S. Shinomori, K. Suzuki, and Y. Arakawa, Phys. Rev. B **58**, R10147 (1998)].

[25] J. D. Mar, X. L. Xu, J. S. Sandhu, A. C. Irvine, M. Hopkinson, and D. A. Williams, Appl. Phys. Lett. **97**, 221108 (2010).

[26] It was assumed that $H = 5$ nm, $z = 33$ nm, and E_b vs V_b were calculated using a 1D self-consistent Poisson-Schrödinger solver. $m_e^* = 0.067m_e$ in GaAs [see S. M. Sze, *Physics of Semiconductor Devices* (Wiley, New York, 1981)], where m_e is the electron mass in vacuum.

[27] P. W. Fry, I. E. Itskevich, D. J. Mowbray, M. S. Skolnick, J. J. Finley, J. A. Barker, E. P. O'Reilly, L. R. Wilson, I. A. Larkin, P. A. Maksym, M. Hopkinson, M. Al-Khafaji, J. P. R. David, A. G. Cullis, G. Hill, and J. C. Clark, Phys. Rev. Lett. **84**, 733 (2000).

[28] X. L. Xu, A. Andreev, and D. A. Williams, New J. Phys. **10**, 053036 (2008).

[29] M. Grundmann, O. Stier, and D. Bimberg, Phys. Rev. B **52**, 11969 (1995).

[30] M. A. Cusack, P. R. Briddon, and M. Jaros, Phys. Rev. B **54**, R2300 (1996).

[31] C. Pryor, Phys. Rev. B **57**, 7190 (1998).

[32] J. Kim, L.-W. Wang, and A. Zunger, Phys. Rev. B **57**, R9408 (1998).

[33] J. J. Finley, M. Sabathil, P. Vogl, G. Abstreiter, R. Oulton, A. I. Tartakovskii, D. J. Mowbray, M. S. Skolnick, S. L. Liew, A. G. Cullis, and M. Hopkinson, Phys. Rev. B **70**, 201308(R) (2004).

[34] J. A. Barker and E. P. O'Reilly, Phys. Rev. B **61**, 13840 (2000).

[35] S. Datta and B. Das, Appl. Phys. Lett. **56**, 665 (1990).

[36] M. Kroner, K. M. Weiss, B. Biedermann, S. Seidl, S. Manus, A. W. Holleitner, A. Badolato, P. M. Petroff, B. D. Gerardot, R. J. Warburton, and K. Karrai, Phys. Rev. Lett. **100**, 156803 (2008).

[37] R. P. G. McNeil, R. J. Schneble, M. Kataoka, C. J. B. Ford, T. Kasama, R. E. Dunin-Borkowski, J. M. Feinberg, R. J. Harrison, C. H. W. Barnes, D. H. Y. Tse, T. Trypiniotis, J. A. C. Bland, D. Anderson, G. A. C. Jones, and M. Pepper, Nano Lett. **10**, 1549 (2010).

[38] J. Berezovsky, M. H. Mikkelsen, N. G. Stoltz, L. A. Coldren, and D. D. Awschalom, Science **320**, 349 (2008).

[39] L. Besombes, J. J. Baumberg, and J. Motohisa, Semicond. Sci. Technol. **19**, S148 (2004).

[40] T. H. Stievater, X. Li, D. G. Steel, D. Gammon, D. S. Katzer, D. Park, C. Piermarocchi, and L. J. Sham, Phys. Rev. Lett. **87**, 133603 (2001).

[41] R. J. Elliott, Phys. Rev. **96**, 266 (1954).

[42] M. I. D'yakonov and V. I. Perel', J. Exp. Theor. Phys. **33**, 1053 (1971).